

Research Article

Fatigue Characteristics of Prestressed Concrete Beam under Freezing and Thawing Cycles

Yuanxun Zheng,¹ Lei Yang,¹ Pan Guo ,^{1,2} and Peibing Yang¹

¹School of Water Conservancy Science and Engineering, Zhengzhou University, Zhengzhou, Henan 450001, China

²School of Civil Engineering, Zhengzhou University, Zhengzhou, Henan 450001, China

Correspondence should be addressed to Pan Guo; 77741289@qq.com

Received 6 July 2020; Revised 31 July 2020; Accepted 23 August 2020; Published 4 September 2020

Academic Editor: Yifeng Ling

Copyright © 2020 Yuanxun Zheng et al. This is an open access article distributed under the Creative Commons Attribution License, which permits unrestricted use, distribution, and reproduction in any medium, provided the original work is properly cited.

In order to reveal the influence of freezing and thawing on fatigue properties of the prestressed concrete beam, a kind of novel freeze-thaw test method for large concrete structure components was proposed, and the freeze-thaw experiments and fatigue failure test of prestressed concrete hollow beams were performed in this paper. Firstly, the compressive strength and dynamic elastic modulus of standard specimens subjected to different numbers of freeze-thaw cycles (0, 50, 75, and 100) were determined. Then, the static and dynamic experiments were performed for prestressed concrete beams under different freeze-thaw cycles. Depending on the static failure test results, the fatigue load for the prestressed concrete beam model was carried out, the fatigue tests for prestressed concrete beam under freezing and thawing cycles were done, and the influence of fatigue loading times on dynamic and static characteristics of prestressed concrete beam was also studied. Finally, the relation between fatigue characteristics and numbers of freeze-thaw cycles was established, and the fatigue life prediction formulas of prestressed concrete beams under freeze-thaw cycles were developed. The research shows that the freezing and thawing cycles had obvious influence on fatigue life, and the freezing and thawing cycles should be taken into account for life prediction and quality evaluation of prestressed concrete beams.

1. Introduction

Because of excellent crack resistance and spanning performance, prestressed concrete structures have been applied extensively in single building structures, highway bridges, offshore, chemical building docks, airports, large tonnage, and other special complex structures. However, prestressed concrete structures inevitably suffer from excessive erosion from the natural environment. In cold climates with greatly contrasting temperatures, concrete bridge structures often experience freeze-thaw damage, which results in the decreased durability of bridges as time progresses, which may eventually lead to the attenuation of the service life of the bridge. Bridge structure disease and collapse accidents have happened caused by freeze-thaw damage in recent decades. Because prestressed concrete bridges have been widely used and assume a vital role in traffic engineering operations, it is

critical to strengthen the freeze-thaw durability of prestressed concrete structures.

Several studies have focused on the frost-resisting performance of prestressed concrete structures. The main theories and academic hypotheses on the mechanisms of concrete freezing and thawing damage are the theory of ice crystal formation, hydrostatic pressure hypothesis, osmotic pressure hypothesis, Litvan freeze-thaw damage theory, critical saturated degree theory, etc. [1]. The most acceptable theories are hydrostatic pressure hypothesis and osmotic pressure hypothesis [2, 3]. He et al. [4] studied the influence of different factors on the temperature field distribution of the slurry in the low-temperature freeze-thaw cycle. The results indicated that several factors such as adding fine aggregate, reducing water-to-cement ratio, and low water content could improve the freeze-thaw cycles resistance of cement-based materials to a certain extent.

Studies have shown that the frost-resisting performance was related to internal pores, water saturation degree, and concrete strength. Hua et al. [5] divided cement mortar specimens into cement mortar and rubber particles, which were, respectively, represented by RSS and CR parameters. Typical correlation method and Szpilman correlation method were used in the analysis. The statistical analysis shows that CR has a high correlation with the residual strength of specimens after freeze-thaw cycle. Jin and Zhao [6] used hydraulic servo test system to test different intermediate stress ratios of 100 mm concrete under triaxial compression. The results show that the triaxial compressive strength is greater than the biaxial compressive strength and uniaxial compressive strength after the same rapid freeze-thaw cycle.

Vesa [7] has statistically studied the deterioration of concrete due to frost action in nonsaline and saline environments. The most significant variables affecting freezing-thawing durability of concrete were calculated statistically and the estimated response surface profile was obtained. The water-cement ratio and air content of concrete are the main factors affecting the internal and surface damage of concrete under freezing-thawing load. On the other hand, Zhao et al. [8] studied the influence of basalt fiber and freeze-thaw cycle on the impact failure mechanism of concrete by means of the concrete beam falling ball impact test. In the early stage of freeze-thaw, the impact energy loss was the fastest and the largest, indicating that freeze-thaw cycle would cause damage and defects to the fiber/matrix interface, thus gradually losing the strengthening effect of three-dimensional fiber system. The experimental study provides a new way to understand the influence of fiber and freeze-thaw cycle on the impact resistance of concrete.

Wu et al. [9] conducted freeze-thaw cycle tests on forty-eight 300 mm cubes of compound concrete and seventy-two 100 mm cubes of FC or demolished concrete, respectively, and determined the compressive failure strength and splitting failure strength of freeze-thaw specimens. With the increase of freeze-thaw cycles, the tensile splitting strength of composite concrete decreases faster than that of FC, while the decline trend of compressive strength is not very obvious. Rui et al. [10] studied the matching of pervious concrete with different matrix types, pore system characteristics, and fiber reinforcement characteristics. The influence of matrix, pore system characteristics, and fiber reinforcement on the freeze-thaw durability of pervious concrete is investigated and potential freeze-thaw failure mechanisms are discussed. Ababneh and Xi [11] proposed an ultrasonic wave model that evaluates concrete salt-freezing damage using pulse velocity and resonant frequency, and the degree of freeze-thaw damage was obtained. Wu et al. [12] regarded mass loss as the variable representing the degree of concrete freeze-thaw damage and proposed a mass loss model. Zhao et al. [13], based on the horizontal strain field on the specimen's surface, a damage degree factor, and a localization factor, proposed to describe the bending damage and failure characteristics of the specimens, with a further analysis of the effect of the fiber content and freeze-thaw cycles on the characteristics. The experimental

results show that the failure process can be divided into three stages: the microfracture dispersion, the macrocrack selection, and the main crack propagation. However, Boyd et al. [14] studied the influence of freeze-thaw metamorphism on the tensile fatigue life of aerated concrete at the initial stage of metamorphism. The results indicated that even though the ultimate static tensile strength of the specimens did not vary significantly due to the freeze-thaw cycles, the residual fatigue properties were degraded. Cho [15] described freeze-thaw damage of concrete using strain change and established a limit function relation between residual strain and the experimental results, and an equivalent plastic strain and its limit state function were established. Peng et al. [16] studied the effect of freeze-thaw cycles on interfacial bonding between concrete and ordinary concrete, high-strength concrete, and additional freeze-resistant concrete by pull-out tests. It is found that the freeze-thaw cycle results in a significant decrease in the compressive strength of ordinary concrete, while the strength of high-strength concrete and concrete mixed with water-reducing agent and air-entraining agent does not. Guo et al. [17] conducted rapid freezing-thawing cycle tests of 0.4, 0.5, and 0.6 water-cement ratios (W/C), respectively, in 0% (water), 1%, and 5% Na_2SO_4 solutions to study the sulfate freezing-thawing cycle performance of ordinary concrete. The results show that, due to the coupling effect of freeze-thaw cycle and sulfate corrosion, the damage of concrete freeze-thaw cycle in Na_2SO_4 solution is greater than that in tap water. Vesikarle [18] obtained the number of frost resistance cycles of concrete by rapid freezing and thawing test cycles, and the service life of concrete was proposed by concrete freeze-thaw cycles fixed in the actual environment every year. Chen et al. [19] conducted experimental research on the degradation of compressive strength of concrete under compressive load and freeze-thaw cycle. The results showed that, based on the degradation model, the freeze-thaw cycle failure evolution model of concrete surface under compression load was established. Wang et al. [20] investigated the loss of shear strength and the mechanism of degradation caused by freeze-thaw cycles through shear tests on the cement-sandstone bonding interface and the material itself. The results show that the shear strength decreases linearly with the increase of freeze-thaw cycles and increases linearly with the increase of normal stress.

In order to effectively evaluate the mechanical properties of concrete after seawater freezing-thawing and seawater erosion, Zhang et al. [21] conducted mechanical properties tests of concrete after seawater freezing-thawing and seawater erosion based on large static and dynamic stiffness servo press. The experimental results show that the compressive strength and elastic modulus of concrete axis gradually decrease and the tensile and compressive meridians of strength criterion gradually shrink with the increase of the cycles of dry and wet cycle and freeze-thaw cycle. Sinha et al. [22] proposed a concrete "deformation uniqueness" in the study of structure fatigue. Matapob [23] described two typical problems of concrete flexural members under repeated load: (1) the influence of steel structure on the strength of flexural reinforced concrete members, crack

formation, and stiffness; (2) some problems on the calculation theory of the fatigue structure of reinforced concrete. Schläfli and Brühwiler [24] conducted a fatigue test on 27 reinforced concrete decks to study the relationship between midspan deflection, concrete strain, and the number of action cycles. Aas-Jakobsen and Lenschow [25] proposed a universal fatigue strength formula for concrete. Furthermore, Tepfers and Kutti [26] perfected the universal fatigue strength formula by a series of tests, and the coefficients were obtained. Zhao [27] performed a test on 16 slabs and analyzed the influence of reinforcement ratio, number of fatigue cycles, and performance of fatigue cycle on fatigue crack, deformation, failure mode, and fatigue resistance capacity of normal section of reinforced concrete slab. Normal section and crack calculation methods for reinforced concrete slab were proposed under fatigue load. Zhao [28] systematically described the fatigue deformation of reinforced concrete and crack and proposed normal section and oblique section fatigue strength models for reinforced concrete and prestressed concrete.

Reinforced concrete tends to suffer internal damage under fatigue actions; that is, it is a period during which fatigue crack brings out, extends, and makes structure broken. The biggest difference between fatigue damage and normal damage is the cumulative fatigue damage period experienced as the load cycles increase. Cheng and Shen [29] pointed out that fatigue lifetime consists of three consecutive stages: fatigue crack formation, fatigue crack propagation, and fatigue damage. Fatigue damage models can be roughly divided into three categories. The first category does not consider the actual performance degradation mechanism for an S-N curve or a similar figure. The second category indicates residual strength. The residual stiffness model of the third category is a damage development model. Yi et al. [30] used linear elastic fracture mechanics to obtain the rotational stiffness expression of the crack section of a concrete member, based on the dynamic test data for four prestressed concrete hollow slabs and their damage performance. Yeo et al. [31] estimated the extent of damage by the static response data of structure. Vestroni and Capecchi [32] identified the damage of structures based on available beam frequency data.

Standard plain concrete or ordinary small reinforced concrete member is gradually becoming the main focus in freeze-thaw and fatigue tests of concrete. Fu [33] performed a fatigue experiment on beams with 0.515 m length which have experienced freeze-thaw erosion, studied component failure mechanism for different freeze-thaw cycles, and discussed the influence of prestressed concrete on freeze-thaw resisting damage as well as the relationship between prestress level, freeze-thaw cycles, and fatigue performance. Lu et al. [34] showed that, for the concrete specimens after exposure to only freeze-thaw cycling or to a combination of freeze-thaw cycles and fatigue loading, with the increase of freezing and thawing cycles, the specimen masses firstly increase and then decrease, whereas the relative dynamical elastic modulus gradually decreases. In addition, Shi et al. [35] points out that the reliability results are in good agreement with the percentile rank method. Furthermore, Liu et al. [36] performed a fatigue test after the prestressed concrete beams experienced several freeze-thaw cycles and analyzed attenuation law of structure stiffness under

fatigue cumulative damage, which states that the greater the number of freeze-thaw cycles is, the more severely beams bend downwards.

To sum up, most of the literatures at home and abroad mainly focus on freeze-thaw cyclic corrosion test or fatigue test on standard ordinary concrete members or ordinary small reinforced concrete members. However, there are few researches on freeze-thaw test and fatigue failure test of prestressed concrete hollow beams with large concrete components. In view of this, a new freeze-thaw test method for large concrete members is presented in this paper, and the freeze-thaw test and fatigue failure test for prestressed concrete hollow beams are carried out. Finally, the relationship between fatigue characteristics and the number of freeze-thaw cycles is established, and the fatigue life prediction formula of prestressed concrete beams under freeze-thaw cycles is established. The freeze-thaw cycle has obvious influence on the fatigue life, so it should be considered in the life prediction and quality evaluation of prestressed concrete beams.

2. Freeze-Thaw Test

2.1. Model Design and Construction. Prestressed concrete hollow beams with concrete grade C50 were used in the test. The mixing proportion of the mixture is shown in Table 1.

The prestressed concrete hollow beam was designed using a 1 × 7 stranded wire with ultimate tensile strength of 1860 MPa, diameter of 12.7 mm, and calculating area of 98.7 mm². The regular reinforcement consists of a longitudinal bar, stirrup, and bearing rod with a diameter of 6 mm. Table 2 summarizes the mechanical property of the regular reinforcement.

The length of the prestressed concrete beam was 2 m with 320 mm height and 500 mm width, while its inner hollow part is 220 mm high and 400 mm wide. There were three prestressed stranded wires in the bottom flange and 16 evenly spaced (100 mm) stirrups in the midspan of the beam. The spacing between the other four stirrups was relatively narrow (50 mm). Figure 1 illustrates the beam section and reinforcement.

2.2. Freeze-Thaw Test and Test Data. Three groups of prestressed concrete beams and C50 concrete cubes were used in the freeze-thaw test. The numbers of freeze-thaw cycles were 50, 75, and 100, respectively. Moreover, an NM-4 A nonmetal ultrasonic detector was used to detect the relative dynamic modulus of elasticity of C50 concrete cubes after the freeze-thaw test. Equations (1) and (2) give the formula of relative dynamic modulus of elasticity [11]:

$$E_d = \frac{(1+v)(1+2v)\rho V^2}{1-v} = \frac{(1+v)(1+2v)\rho L^2}{(1-v)t^2}, \quad (1)$$

$$E_{rd} = \frac{E_{dt}}{E_{d0}} = \frac{V_t^2}{V_0^2} = \left(\frac{T_0}{T_t}\right)^2, \quad (2)$$

where E_d is the dynamic modulus of elasticity, v is Poisson's ratio, ρ is the concrete density (kg/cm³), L is the length of

TABLE 1: Concrete mixing proportion.

Cement	Fly ash	River sand	Macadam	Polycarboxylic acid type water-reducer	Water
450	50	722	1035	5	160

TABLE 2: Ordinary steel mechanical property.

Reinforcement	Tensile strength design value (MPa)	Compressive strength design value (MPa)	Elastic modulus (ep)
Φ6	330	330	2.0×10^5

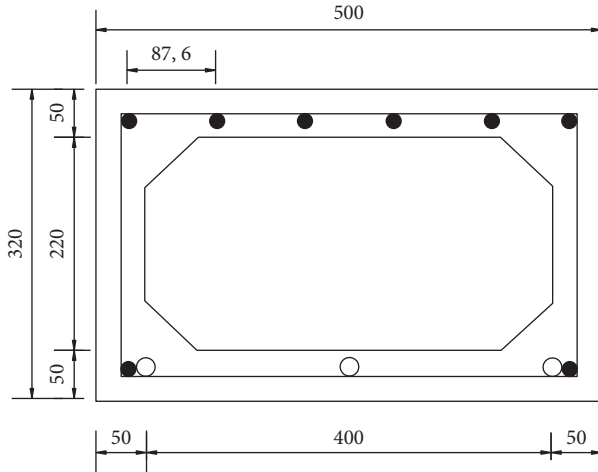


FIGURE 1: Beam section and reinforcement (unit: mm).

component (m), t is the propagation time of ultrasonic testing (μs), E_{rd} is the relative dynamic modulus of elasticity, T_0 is the propagation time of ultrasonic testing in concrete cube before erosion, and T_t is the propagation time of ultrasonic testing in concrete cube after erosion. During the erosion process, Poisson's ratio ν of concrete is insensitive and changes slightly.

Pressure testing machine was used to test the compressive strength of C50 concrete cubes, which is computed by the following equation [37]:

$$f_c = 0.95 \frac{F}{A}, \quad (3)$$

where f_c is the compressive strength of concrete cube, F is the failure load, and A is the pressure-bearing area.

Tables 3 and 4 summarize the relative dynamic elastic modulus and compressive strength data, respectively.

According to Table 3, the relative dynamic elastic modulus of the same C50 concrete reduced as the number of freeze-thaw cycles increased, and the speed of ultrasonic wave through C50 concrete reduced. The internal parts of the concrete begin to experience gradual increase in damage as freeze-thaw cycles increase.

3. Fatigue Load Experiment

3.1. Static Load Test. Static load test was performed before fatigue load experiment to determine the ultimate bearing capacity of prestressed concrete beam. Based on the ultimate bearing capacity, the fatigue stress ratio was determined as

0.8 [38]. Figures 2 and 3 illustrate the schematic of static load test and actual device, respectively.

Prestressed concrete hollow slab shows large deformation, and the upper concrete is nearly broken when the static load is 200 kN. The static load changes slowly on the specimen when it is 200–245 kN. But when the load is up to 245 kN, the specimen is completely crushed, and the displacement of midspan part changes acutely. In view of the experiment phenomenon and the related strain deflection data, the ultimate limit fracture of the test beam is $P_{max} = 200$ kN.

3.2. Fatigue Cycle Test. Fatigue load experiments were performed on beams that experienced 0, 50, 75, and 100 freeze-thaw cycles. Figure 2 illustrates the load method, while Table 5 summarizes the fatigue limit load and load frequency.

The fatigue test was performed using a hydraulic fatigue testing machine. The dynamic performance tests were carried out after 5.0×10^5 fatigue load times. The appearance and development of crack were observed continually, and the component was considered as failure and the test was stopped when the crack width was up to 0.2 mm. As shown in Figures 4 and 5, the electronic strain gauges and vibration pickups were used to collect test data.

3.3. Data and Analysis of Fatigue Test Results

3.3.1. Numbers of Failure Fatigue Load Actions and Cracking Load Actions. As the freeze-thaw cycles increased, the crack width was up to 0.2 mm and the test was stopped. The numbers of failure fatigue load and cracking load actions differed when four groups of prestressed concrete beams cracked. Figures 6 and 7 illustrate the numbers of cracking load actions and failure fatigue load actions, respectively.

In Figure 6, the number of cracking load actions decreased as the freeze-thaw cycles increased. Comparing 50 freeze-thaw cycles with 75 freeze-thaw cycles, the number of cracking load actions decreased slowly, while the number of cracking load actions of beams that experienced 100 freeze-thaw cycles decreased rapidly.

These phenomena indicate that the beams cracked before the freeze-thaw cycles increased such that the crack resistance of the beams decreased very rapidly after relative multiple freeze-thaw cycles equal to the number of failure fatigue load actions. In Figure 7, the increase in freeze-thaw

TABLE 3: Relative dynamic elastic modulus of concrete cubes experiencing different freeze-thaw cycles.

Number of freeze-thaw cycles	Relative dynamic elastic modulus (%)
0	100
50	87.1
75	84.9
100	78.6

TABLE 4: Average compressive strength of concrete cubes experiencing different freeze-thaw cycles.

Number of freeze-thaw cycles	Average fracture load (kN)	Average compressive strength (\bar{f}_{cu})
0	553.600	52.59
50	482.000	45.79
75	471.300	44.77
100	455.500	43.27

cycles led to a decrease in the fatigue life. The cracking load action has a similar degradation rule.

3.3.2. Data of Static Load after Fatigue Action.

Freeze-thaw cycles are a variable of fatigue loading causing accumulated damage. Static and dynamic load tests after 5.0×10^5 fatigue load actions are means of monitoring the beam performance. A fatigue experiment was carried out for four groups of prestressed concrete beams, where the numbers of loading actions are 0, 5.0×10^5 , and 1.0×10^6 . A level 3 loading test was then performed, where the loads are 5 ton, 10 ton, and 15 ton. Figure 8 illustrates the midspan compressive strain for different freeze-thaw cycles before fatigue action, while Figure 9 illustrates the midspan tensile strain for different freeze-thaw cycles before fatigue action. Figure 10 illustrates the midspan displacement for different freeze-thaw cycles before fatigue action.

Figure 8 illustrates that the force made frost heave cracks close gradually in the compressive zone as the freeze-thaw cycles increased, thereby resulting in an increase in the concrete compressive strain. Comparing the results of 0, 50, and 100 freeze-thaw cycles with 50, 75, and 100 freeze-thaw cycles, the increase in freeze-thaw cycles accelerated the increase in compressive strain of concrete at the upper flange plate of the beam.

In Figure 9, compared with beam that never suffered freeze-thaw cycles, tensile strain increment of the beam's lower flange plate that suffered different freeze-thaw cycles is little. The results of 50 and 75 freeze-thaw cycles have same parts, and the results of 100 freeze-thaw cycles are evident. But range ability is not rapid as compressive strain. Meanwhile, the expansion coefficients of concrete and steel are similar. Hence, the influence of freeze-thaw actions on cementing action between prestressed wire and concrete is insignificant.

Data acquisition and data processing were carried out after every 5.0×10^5 fatigue action cycles. The same-level load (15 tons) was selected to observe the change in the strain of

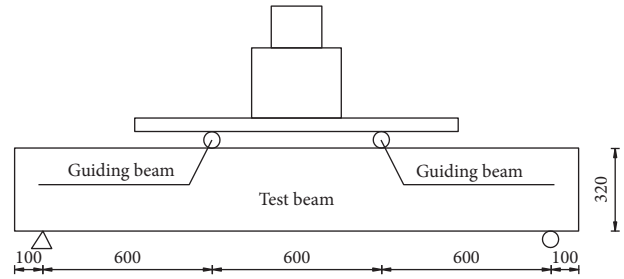


FIGURE 2: Schematic diagram of static load (unit: mm).



FIGURE 3: Loading equipment and methods of static load.

TABLE 5: Fatigue limit load and load frequency.

Specimen number	Maximum fatigue load F'_{max} (kN)	Minimum fatigue load F'_{min} (kN)	Frequency (Hz)
D-0	160	60	5
D-50	160	60	5
D-75	160	60	5
D-100	160	60	5

beam. The beams used in all the tests below suffered different freeze-thaw cycles and then suffered fatigue action. Figure 11 illustrates the midspan strain of the beam's upper flange plate, whereas Figure 12 illustrates the change in midspan tensile strain of the beam's lower flange plate. Moreover, Figure 13 illustrates the change in midspan displacement of the beam's lower flange plate, whereas Figure 14 illustrates the change in compressive strain of the beam's upper 1/4 part. In addition, Figure 15 illustrates the change in tensile strain of the lower 1/4 part of the beam, whereas Figure 16 illustrates the change in the midspan displacement of the lower 1/4 flange plate of the beam.

From Figures 11–15, the following can be observed: (1) The strain and displacement of prestressed concrete beams that experienced freeze-thaw cycles were larger in comparison with the prestressed concrete beams that did not experience freeze-thaw cycles. In this situation, the change in compressive strain of the midspan part of the beam is evident. The compressive strain increased as the freeze-thaw cycles increased such that the compressive strain increased rapidly for 50 freeze-thaw cycles. This tendency is mainly reflected in the static load test on the test beams with different freeze-thaw cycles (50, 75, and 100 times). The

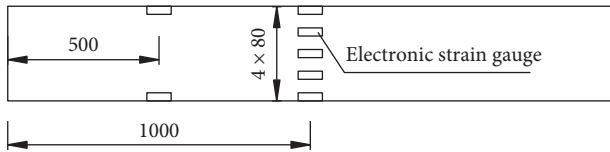


FIGURE 4: Longitudinal view of the electronic strain gauge location (unit: mm).

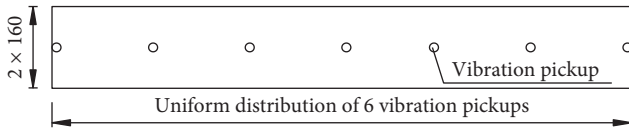


FIGURE 5: Location of vibration pickup in top area (unit: mm).

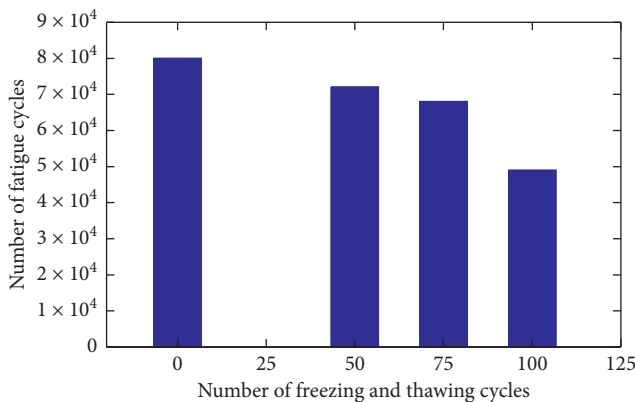


FIGURE 6: Fatigue loading times of beams with different freeze-thaw cycles.

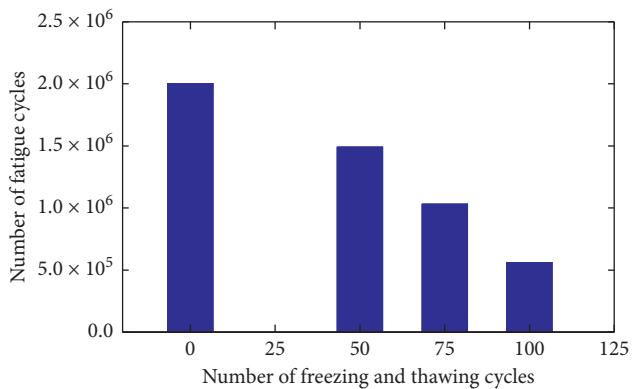


FIGURE 7: Fatigue loading times of beams with different freeze-thaw cycles.

different freeze-thaw cycles the beam suffers, the more the number of freeze-thaw cycles is and the bigger the compressive strain is. Moreover, the compressive strain increases considerably as the freeze-thaw cycles increase similar to midspan displacement. Thus, the compressive strain of the beam's upper flange plate increased as the number of freeze-thaw cycles increased. For 5.0×10^5 fatigue loading actions, the strain increases rapidly as the beam suffers 100 freeze-

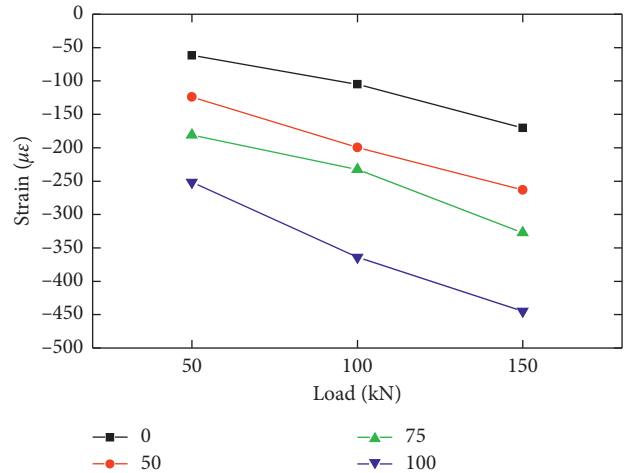


FIGURE 8: Compressive strain at the top of the test beam under three-stage loading for different freeze-thaw cycles before fatigue.

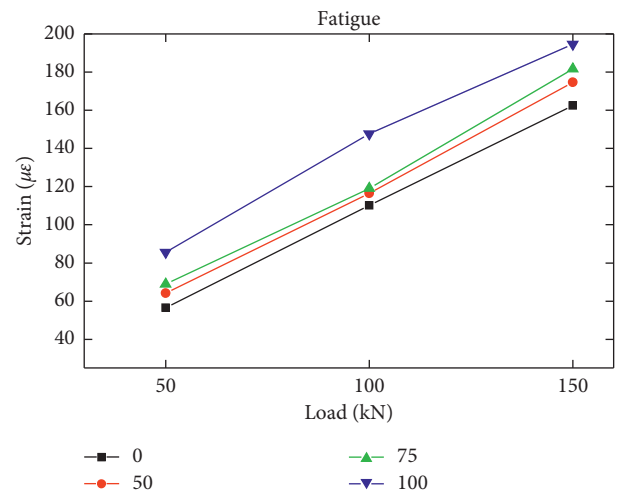


FIGURE 9: Different freeze-thaw cycles before fatigue test load under tensile strain beam span.

thaw cycles. This may be due to the development of cracks or concrete failure. (2) Considering the tensile strain in the midspan and 1/4 bottom part of the beam, the bottom strain of four groups of beams increases slightly. In Figure 12, when fatigue loading actions reach 1.0×10^6 times, the difference that freeze-thaw cycles lead to is evident compared with the midspan tensile strain. Thus, the change rule of tensile strain of the beam's 1/4 parts is not evident. (3) In Figures 13 and 16, the beam displacement increased as the freeze-thaw cycles increased, thereby indicating that the influence of freeze-thaw cycles on the bending performance of beam is high. For example, the midspan displacement of the test beams with the same fatigue times increases gradually with the increase of freeze-thaw times.

To study the influence of freeze-thaw cycles on strain and displacement of beam comprehensively, four groups of beams were prepared as a test object, based on the condition that the smallest number of fatigue failure loads is 5.0×10^5 . To study the compressive strain at the top midspan of the

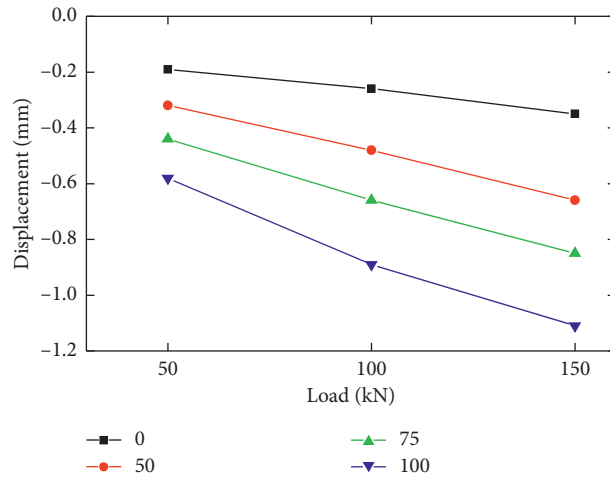


FIGURE 10: Midspan displacement under three-stage load of test beam for different freeze-thaw cycles before fatigue.

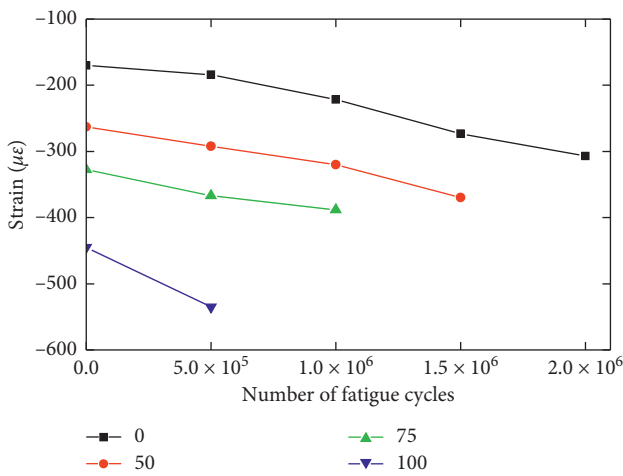


FIGURE 11: Compressive strain at the top of the span under fatigue action of test beams for different freeze-thaw cycles.

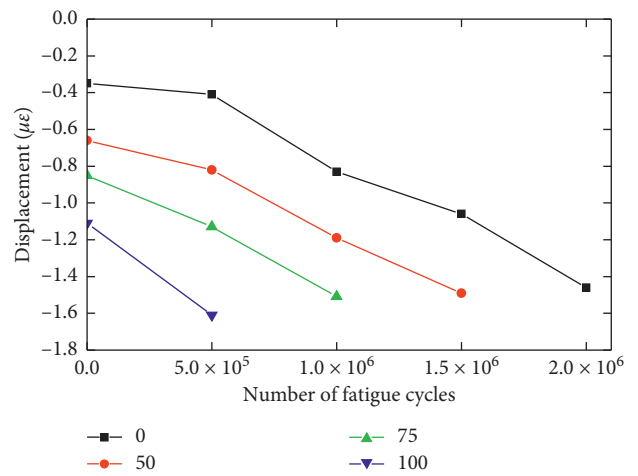


FIGURE 13: Midspan displacement of test beams subjected to fatigue for different freeze-thaw cycles.

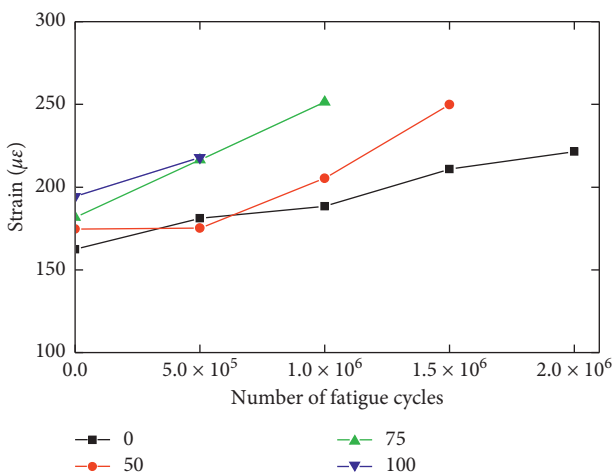


FIGURE 12: Tensile strain at the bottom of the span under fatigue action of test beams for different freeze-thaw cycles.

beam and displacement at the bottom midspan of the beam, the number of fatigue loading actions of beam ranges from 0 to 5.0×10^5 . Figure 17 illustrates the percentage of increase of compressive strain at the top midspan of the beam, while Figure 18 illustrates the percentage of increase of displacement at the bottom midspan of the beam.

In Figure 17, an expression could be obtained using the number of freeze-thaw cycles N and percentage of increase Y as follows:

$$50\text{--}75 \text{ freeze-thaw cycles: } Y_2 = 0.000383539N.$$

$$75\text{--}100 \text{ freeze-thaw cycles: } Y_3 = 0.003262578N.$$

In Figure 18, an expression could be obtained using the number of freeze-thaw cycles N and percentage of increase Y as follows:

$$50\text{--}75 \text{ freeze-thaw cycles: } Y = 0.319714795N$$

$$75\text{--}100 \text{ freeze-thaw cycles: } Y = 0.43727398N$$

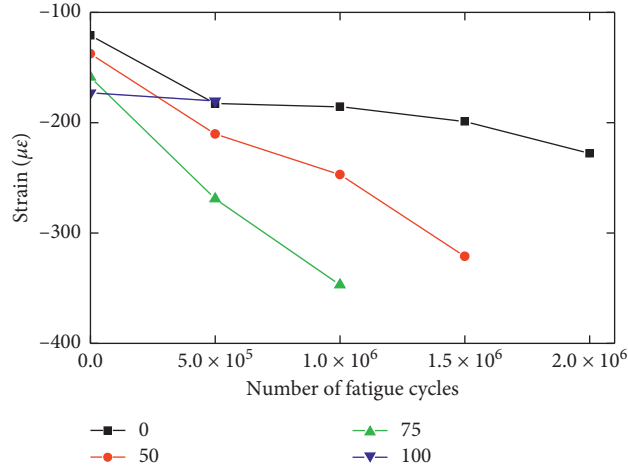


FIGURE 14: Compressive strain at the top of 1/4 test beams for different freeze-thaw cycles.

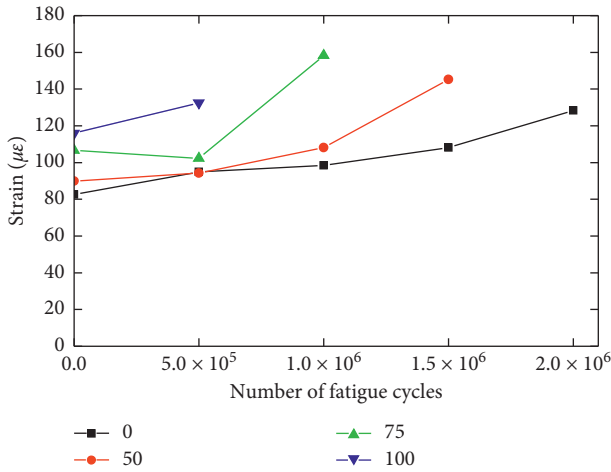


FIGURE 15: Tensile strain at the bottom of 1/4 test beams subjected to fatigue for different freeze-thaw cycles.

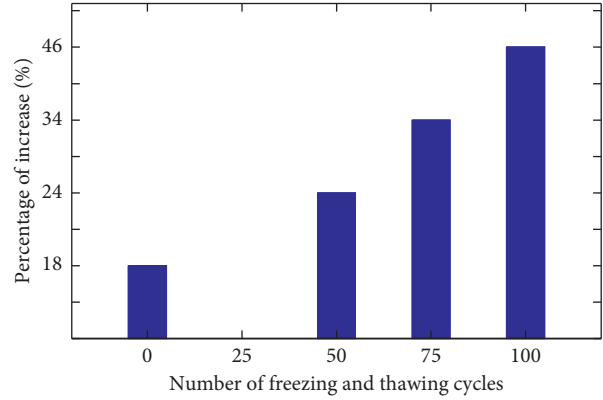


FIGURE 17: Percentage of increase of compressive strain of test beam from 0 to 5.0×10^5 times for different freeze-thaw cycles.

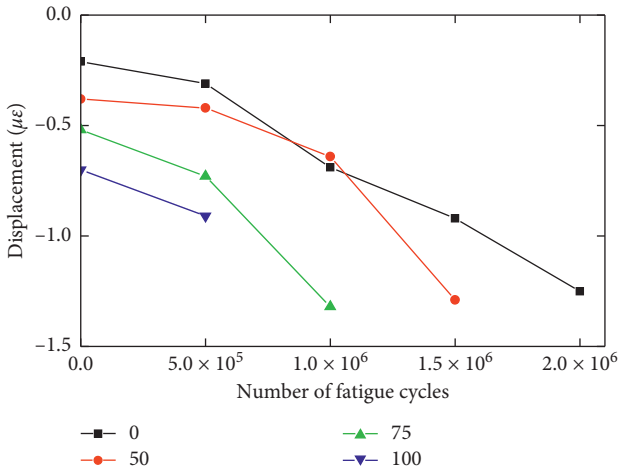


FIGURE 16: 1/4 displacement of test beams subjected to fatigue for different freeze-thaw cycles.

In Figures 17 and 18, the two groups of histograms show an increasing trend. The slope of the expression increased and indicated that the beam's compressive strain increased significantly as the freeze-thaw cycles increased. This proves that the failure of the upper parts of the beam develops rapidly with the increase in freeze-thaw cycles under the same fatigue actions, the midspan displacement significantly increases, and downwarping occurs increasingly quickly. These are similar to the situation where the amount of failure fatigue load and the amount of cracking load decrease.

3.3.3. *Dynamic Load Results after Fatigue Load.* The dynamic load test includes a frequency test and dynamic displacement test, daubing the yellow grease on the bottom of vibratory sensors. The vibratory sensors were placed in a similar way to that in Figure 5, and the results are illustrated in Figure 19. Strain and displacement were measured in the same manner. Moreover, an ultrasonic acquiring instrument with a collecting frequency of 50 Hz was used in the displacement test, where the test probes were placed at the bottom and center of the beam. Then, a signal acquiring instrument that was developed by Beijing Oriental Institute

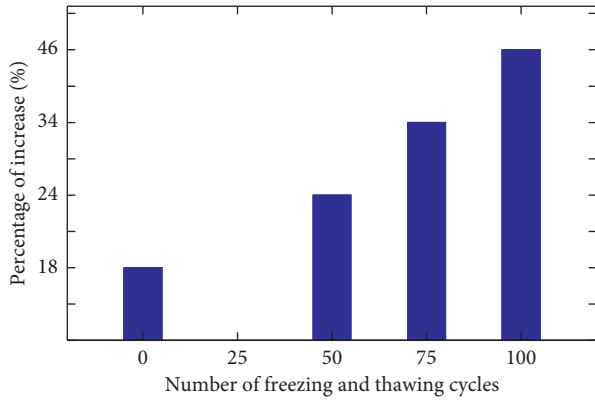


FIGURE 18: Percentage of increase of displacement test beam from 0 to 5.0×10^5 times for different freeze-thaw cycles.

of Technology was used to capture vibration and noise. The test was then performed under fatigue loading actions, and the results are illustrated in Figure 20.

The natural frequency decreased as the fatigue loading actions increased and decreased as the freeze-thaw cycles increased. In Figure 20, the crest value of dynamic displacement increased after experiencing frost erosion and after fatigue action for the same freeze-thaw cycles.

4. Conclusions

- (1) As the freeze-thaw cycles increase, the time point of crack failure of prestressed concrete beams crack after freeze-thaw cycles under fatigue actions is earlier than that of the beam without freeze-thaw cycles. Furthermore, the speed of development of the beam's fatigue cracks is faster than that in the beam that never suffered frost erosion.
- (2) As the freeze-thaw cycles increase for the same number of fatigue loading actions, the compressive strain at the upper flange plate and the tensile strain at the lower flange plate of the beam increase. Moreover, as the number of freeze-thaw cycles increases further, this tendency increases faster. The change in the compressive strain at the upper flange plate is significant. However, the change in tensile strain is insignificant before 1.0×10^6 fatigue actions and gradually becomes significant after 1.0×10^6 fatigue actions.
- (3) The beam's midspan displacement increases during this process. Thus, freeze-thaw cycles have an influence on the blending resistance performance of the test beam and accelerate the decrease in the stiffness of the beam.
- (4) Based on the strain and displacement histograms and by fitting linear formula, we can see that, with an increase in freeze-thaw cycles under the same fatigue loading action, the compressive strain at the upper flange plate and displacement of midspan tend to increase. The compressive strain progressively increases, which proves that the modulus of elasticity

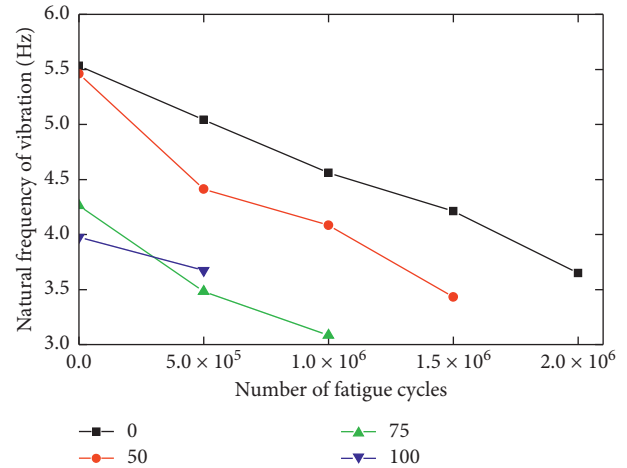


FIGURE 19: Fundamental frequency value of different freeze-thaw cycle test beams under fatigue action.

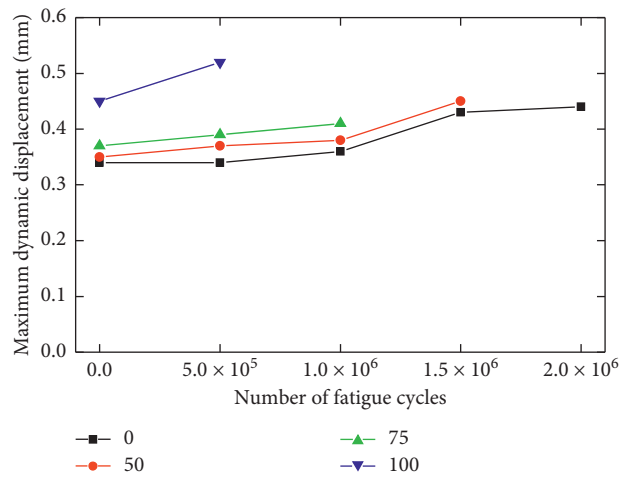


FIGURE 20: Peak value of dynamic displacement wave under fatigue action of test beams for different freeze-thaw cycles.

decreases after the freeze-thaw cycles. Although the freeze-thaw cycles accelerate the degree of deflection, the increasing speed of displacement is lower than the increasing speed of compressive strain. Thus, the prestressed concrete beam's health decreases.

- (5) Depending on the data of the beam natural frequency test, the natural frequency of the beams decreases as the freeze-thaw cycles increase, as damage occurs in the beam's internal parts when stiffness decreases during the frost period. Meanwhile, cracks occur in the beam under fatigue loading actions. These cracks develop further, thereby leading to a decrease in the bearing capacity and stiffness of the beam. Thus, the natural frequency decreases.

Data Availability

The data used to support the findings of this study are included within the article.

Conflicts of Interest

The authors declare that they have no conflicts of interest.

Acknowledgments

This work was supported by the Natural Science Foundation of Henan (Grant No. 51508114), Science and Technology Program of the Communications Department of Henan Province (Grant No. 2014K37-2), Foundation Sponsored by Program for Science and Technology Innovation Talents in Universities of Henan Province (Grant No. 16HASTIT012), and Outstanding Young Talent Research Fund of Zhengzhou University (Grant No. 4). The authors acknowledge the test field support of the Communications Department of Henan Province and also acknowledge the advice and support of Dr. Pan Ernian of the University of Akron.

References

- [1] X. Liu and G. Tang, "Research on prediction method of concrete freeze-thaw durability under field environment," *Chinese Journal of Rock and Mechanics and Engineering*, vol. 26, no. 12, pp. 2412–2419, 2007.
- [2] T. C. PoWers, "A working hypothesis for further studies of frost resistance," *Journal of the American Concrete Institute*, vol. 16, no. 4, pp. 245–272, 1945.
- [3] T. C. PoWers and H. El Muthra, "Theory of volume change in hardened portland cement paste during freezing," *Highway Research Board*, vol. 32, pp. 85–21, 1953.
- [4] B. He, MingjunXie, Z. Jiang, C. Zhang, and XipingZhu, "Temperature field distribution and microstructure of cement-based materials under cryogenic freeze-thaw cycles," *Construction and Building Materials*, vol. 234, pp. 1–14, 2020.
- [5] L. Hua, "A potential damage mechanism of rubberized cement under freeze-thaw cycle," *Construction and Building Materials*, vol. 252, pp. 1–12, 2020.
- [6] W. Jin and Y. Zhao, "The Durability of Concrete Structure," Science Press, Beijing, China, 2002.
- [7] V. Penttala, "Surface and internal deterioration of concrete due to saline and non-saline freeze-thaw loads," *Cement and Concrete Research*, vol. 36, no. 5, pp. 921–928, 2006.
- [8] Y.-R. Zhao, L. Wang, Z.-K. Lei, X.-F. Han, and Y.-M. Xing, "Experimental study on dynamic mechanical properties of the basalt fiber reinforced concrete after the freeze-thaw based on the digital image correlation method," *Construction and Building Materials*, vol. 147, pp. 194–202, 2017.
- [9] B. Wu and Z. Li, "Mechanical properties of compound concrete containing demolished concrete lumps after freeze-thaw cycles," *Construction and Building Materials*, vol. 155, pp. 187–199, 2017.
- [10] R. Zhong and K. Wille, "Influence of matrix and pore system characteristics on the durability of pervious concrete," *Construction and Building Materials*, vol. 162, pp. 132–141, 2018.
- [11] A. N. Ababneh and Y. Xi, "Evaluation of environmental degradation of concrete in cold regions," in *Proceedings of the 13th International Conference on Cold Regions Engineering*, American Society of Civil Engineers, Orono, ME, USA, pp. 1–10, July 2006.
- [12] Q. Wu, H. Yu, and X. Chen, "A Service life prediction method of concretes based on mass loss rate: establishment and narration of mathematical model," in *Proceedings of the 10th International Conference of Chinese Transportation Professionals*, American Society of Civil Engineers, Beijing, China, pp. 3253–3260, August 2010.
- [13] Y.-R. Zhao, L. Wang, Z.-K. Lei, X.-F. Han, and J.-N. Shi, "Study on bending damage and failure of basalt fiber reinforced concrete under freeze-thaw cycles," *Construction and Building Materials*, vol. 163, pp. 460–470, 2018.
- [14] A. J. Boyd and A. Leone, "Effect of freeze-thaw cycling on fatigue behaviour in concrete," *Materials Science and Engineering*, vol. 652, pp. 1–6, 2019.
- [15] T. Cho, "Prediction of cyclic freeze-thaw damage in concrete structures based on response surface method," *Construction and Building Materials*, vol. 21, no. 12, pp. 2031–2040, 2007.
- [16] H. Peng, F. Asce, J. Yu, and J. Zhang, "Experimental investigation of bond between near-surface-mounted cfrp strips and concrete under freeze-thawing cycling," *American Society of Civil Engineers*, vol. 32, no. 1, Article ID 4018125, 2019.
- [17] Li Guo, D. U. Jian Min, X. S. Wu, and K. Yang, "Resistance of concrete to Na₂SO₄ freeze-thaw cycles and failure mechanism analysis," *Key Engineering Materials*, vol. 711, pp. 335–342, 2016.
- [18] E. Vesikarle, "Service Life Design of Concrete Structure with Regard to Frost Resistance of Concrete," pp. 215–228, Nordic Concrete Research, Oslo, Norway, 2018.
- [19] S. Chen, X. Song, and X. Liu, "Compressive strength degradation and evolution of failure surfaces in compressively preloaded concrete under freeze-thaw cycles," *Materials Research Innovations*, vol. 19, pp. 433–437, 2015.
- [20] W. Wang, X. Yang, S. Huang, D. Yin, and G. Liu, "Experimental study on the shear behavior of the bonding interface between sandstone and cement mortar under freeze-thaw," *Rock Mechanics and Rock Engineering*, vol. 53, no. 2, pp. 881–907, 2019.
- [21] F. Zhang, S. Li, J. Ye, and S. Li, "Evolution model of concrete failure surface under coupling effect of seawater freeze-thaw and erosion," *Journal of Southeast University(English Edition)*, vol. 27, no. 2, pp. 206–209, 2011.
- [22] B. P. Sinha, K. H. Gcrstlc, and L. G. Tulin, "Stress-strain relations for concrete under cyclic loading," *ACI Journal*, vol. 61, no. 2, pp. 195–211, 2014.
- [23] H. A. Matapob, "Performance Research of Reinforced Concrete Flexural Members Performance Study," Beijing: Science Press, Beijing, China, 1964.
- [24] M. Schläfli and E. Brühwiler, "Fatigue of existing reinforced concrete bridge deck slabs," *Engineering Structures*, vol. 20, no. 11, pp. 991–998, 1998.
- [25] K. Aas-Jakobsen and R. Lenschow, "Behavior of reinforced columns subjected to fatigue loading," *Journal of the American Concrete Institute*, vol. 70, no. 3, pp. 199–206, 1973.
- [26] R. Tepfers and T. Kutti, "Fatigue strength of plan, ordinary, and lightweight concrete," *Journal of the American Concrete Institute*, vol. 76, no. 5, pp. 199–206, 1979.
- [27] S. Zhao, "Experimental study on fatigue behaviors of reinforced concrete plates," *Journal of Basic Science and Engineering*, vol. 7, no. 3, pp. 289–297, 1999.
- [28] G. Zhao, *High Reinforced Concrete Structural Study*, China Electric Power Press, Beijing, China, 1999.
- [29] Yi Cheng and S. Shen, "The fatigue crack propagation laws and their application in the research on fatigue property of concrete," *Journal of Harbin University of Civil Engineering & Architecture*, vol. 33, no. 5, pp. 20–24, 2000, in Chinese.
- [30] W. Yi, C. Wang, and P. Shen, "Actual vibration test examples of concrete structures and their analysis," *Journal of Hunan University*, vol. 22, no. 3, pp. 96–103, 1995.

- [31] I. Yeo, S. Shin, H. S. Lee, and S.-P. Chang, "Statistical damage assessment of framed structures from static responses," *Journal of Engineering Mechanics*, vol. 126, no. 4, pp. 414–421, 2000.
- [32] F. Vestroni and D. Capecchi, "Damage detection in beam structures based on frequency measurements," *Journal of Engineering Mechanics*, vol. 126, no. 7, pp. 761–768, 2000.
- [33] K. Fu, "The fatigue properties of prestressed concrete structure in an erosion environment with fatigue subjoining freezing-thawing circle," Master thesis, Zhenjiang: Faculty of Civil Engineering and Mechanics, Zhenjiang, China, 2008.
- [34] J. Lu, L. Tian, L. Tong, and K. Zhu, "Dynamic properties of concrete subjected to combined action of fatigue load and freeze-thaw cycles," *Journal of Biomechanical Science and Engineering*, vol. 26, no. 5, pp. 1055–1066, 2018.
- [35] K. Shi, Y. Zhang, X. Wang, and Y. Dai, "Analysis of reliability of pre-stressed concrete fatigue system in freezing and thawing environment based on Monte Carlo method," *Journal of Jiangsu University of Science and Technology (Natural Science Edition)*, vol. 32, no. 5, pp. 740–745, 2018.
- [36] R. Liu, Y. Zhang, and Y. Chen, "Fatigue damage model of prestressed concrete beams suffered freeze–thawing," *Journal Of Jiangsu University (Natural Science Edition)*, vol. 33, no. 1, pp. 115–119, 2012.
- [37] "Standard for test methods for physical and mechanical properties of concrete," 2019.
- [38] X. Zhao, X. Wang, Z. Wu, and Z. Zhu, "Fatigue behavior and failure mechanism of basalt FRP composites under long-term cyclic loads," *International Journal of Fatigue*, vol. 88, pp. 58–67, 2016.